SUPPLEMENTAL METHODS

QUINONE ANALYSES

Separation by HPLC – Ubiquinones of different polyprenyl-chain length (Q_1, Q_6, Q_{10}; from Sigma) were separated on a reversed-phase column (EC 250/4.6 Nucleosil 300-5 C8, Macherey Nagel) connected to an Agilent 1100 HPLC system (Hewlett Packard) at 40 °C and a flow rate of 0.8 ml min^{-1}. Quinones were monitored by measuring the absorbance at 275 nm. A gradient from 60-100% methanol allowed separating Q_1 (8.0-9.0 min elution time), Q_2 (14.5-15.5 min), and 2-N_3-Q_2 or 3-N_3-Q_2 (16.5-17.0 min). A gradient from 80-100% methanol led to separation of Q_6 (18.3 min), Q_8 (22.3-23.4 min), and Q_{10} (26.7 min). Na^+ -NQR purified in *n*-dodecyl-β-D-maltoside (DDM; Glycon) contained 0.68 mol ubiquinone-8 per mol Na^+ -NQR. Na^+ -NQR purified in lauryldimethylamine *N*-oxide (LDAO; Glycon) did not contain any quinones (Fig. S1).

Identification of ubiquinone-8 by mass spectroscopy – ESI-MS analysis of quinones was performed on a Q-TOF Ultima instrument (Waters) equipped with a nano-ESI-source and controlled by the MassLynx software (Waters). Samples were applied by direct infusion at 1 µl min^{-1}. The capillary voltage was set to 3.5 kV and the collision energy was set to 10 eV. Data were collected in the centroid mode. The instrument was calibrated with [Glu^1]•fibrinopeptide B ($[M]^{2+}$: 785.842 Da theoretical, 785.820 Da observed; from Sigma). H^+ and Na^+ adducts of Q_{10} standards (in methanol containing 0.1% formic acid) were observed ($[Q_{10}•H]^+$: 863.692 Da theoretical, 863.672 Da observed; $[Q_{10}•Na]^+$: 885.674 Da theoretical, 885.645 Da observed). Quinones present in the organic extract of the Na^+-NQR after metal affinity and size exclusion chromatography in DDM were separated by HPLC. ESI-MS analysis of the major fraction eluting at 23.4 min confirmed that the quinone bound to the Na^+ -NQR is Q_8 (Fig. S2). A major compound with a mass to charge ratio (m/z) of 749.536 Da and a minor compound with m/z of 727.554 Da were observed. These values corresponded to the Na^+ and H^+ adducts of Q_8, which have calculated masses of 749.549 Da and 727.567 Da, respectively.

SUPPLEMENTAL TABLE

TABLE S1: Chemical shifts of Q_1 and HQNO. Ubiquinone-1 (Q_1) or 2-*n*-heptyl-4-hydroxyquinoline *N*-oxide (HQNO) in DMSO-d6 was diluted twofold in D_2O containing 10 mM potassium phosphate, pH 8.0, 150 mM NaCl, 4 mM NaN_3. The final concentration was 10 mM. ^1H, ^1H-^{13}C-HSQC, ^1H-^{13}C-HMBC and 2D-NOESY NMR spectra were recorded at 300 K.

Q_1						
Atoms	2,3 CH_3-O	H5' / C5'	H7 / C7	H8 / C8	H10 / C10	H11 / C11
δ $^1H/^{13}C$, ppm	3.81 61.0	2.51 38.3	3.04 24.7	4.83 119.0	1.61 17.4	1.51 25.1
HQNO						
Atoms	H3 / C3	H5 / C5	H6 / C6	H7 / C7	H8 / C8	H11 / C11
δ $^1H/^{13}C$, ppm	6.10 105.9	8.08 124.7	7.36 124.0	7.66 131.3	8.05 116.8	2.75 30.9
Atoms	H12 / C12	H12 / C12	H13 / C13	H14 / C14	H15 / C15	H16 / C16
δ $^1H/^{13}C$, ppm	1.61 27.1	1.27 28.5	1.27 28.5	1.20 31.1	1.20 22.2	0.79 14.1

SUPPLEMENTAL FIGURES

FIGURE S1: Quinone depletion of Na^+-NQR after treatment with LDAO. HPLC elution profiles of organic extracts from Na^+-NQR in DDM (728 µg, dashed trace) and in LDAO (603 µg, solid trace). Q_8 elutes at 23.5 min.

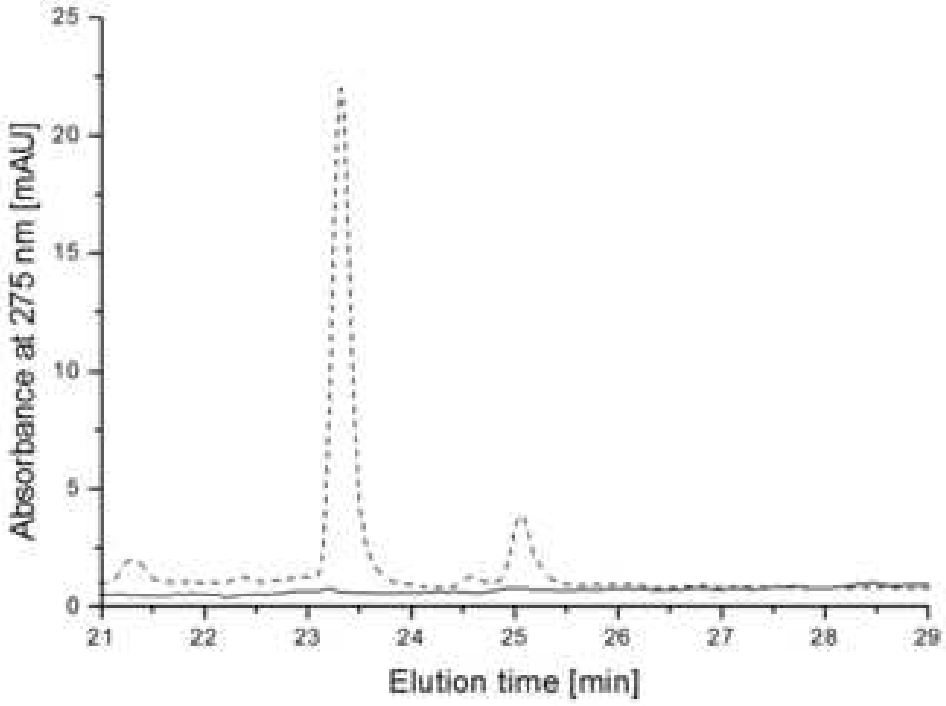

FIGURE S2:ESI-MS analysis of ubiquinone. MS spectra of HPLC-purified quinone (peak at 23.4 min, see Fig. S1) extracted from purified Na^+-NQR (A). Simulated spectra of $[Q_8•H]^+$ (B) and $[Q_8•Na]^+$ (C).

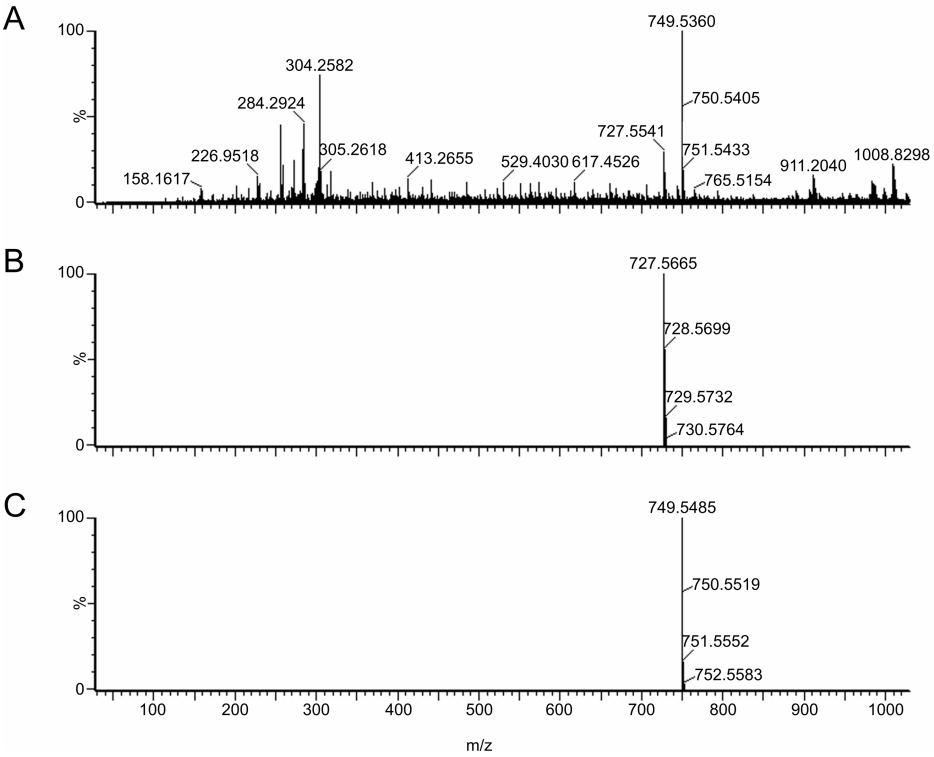

FIGURE S3: Binding of quinone derivatives to Na^+-NQR and subunit NqrA. Quinone-depleted Na^+-NQR (200-400 µg) or NqrA (220-280 µg) was incubated with quinone derivatives and purified by Ni-chromatography. Organic extracts of reconstituted protein were analysed for bound quinone by HPLC. Chromatogram of Q_1 co-purified with Na^+-NQR (blue trace) or NqrA (red trace), respectively, and chromatogram of Q_1 standard (black trace) (A). Chromatogram of Q_2 co-purified with Na^+-NQR (blue trace) or NqrA (red trace), respectively, and chromatogram of Q_2 standard (black trace) (B). Chromatogram of 2-N_3-Q_2 (blue trace) and 3-N_3-Q_2 (red trace), respectively, co-purified with Na^+-NQR, and chromatogram of 2-N_3-Q_2 standard (black trace) (C).

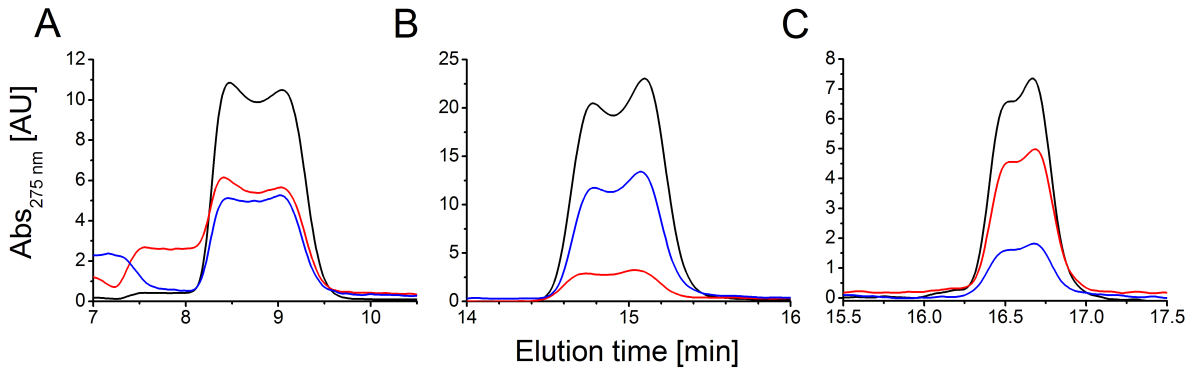

FIGURE S4: MALDI-MS spectra of Na^+-NQR. MS-spectra were obtained from Na^+-NQR illuminated in the presence of Q_1 (A) and 3-N_3-Q_2 (B), respectively. The m/z values of peaks labeled a to l are given in Table 1. (C), the m/z range from 50 to 55 kD of the spectra from the Q_1 treated protein (solid line) and the 3-N_3-Q_2 treated protein (dashed line) are compared.

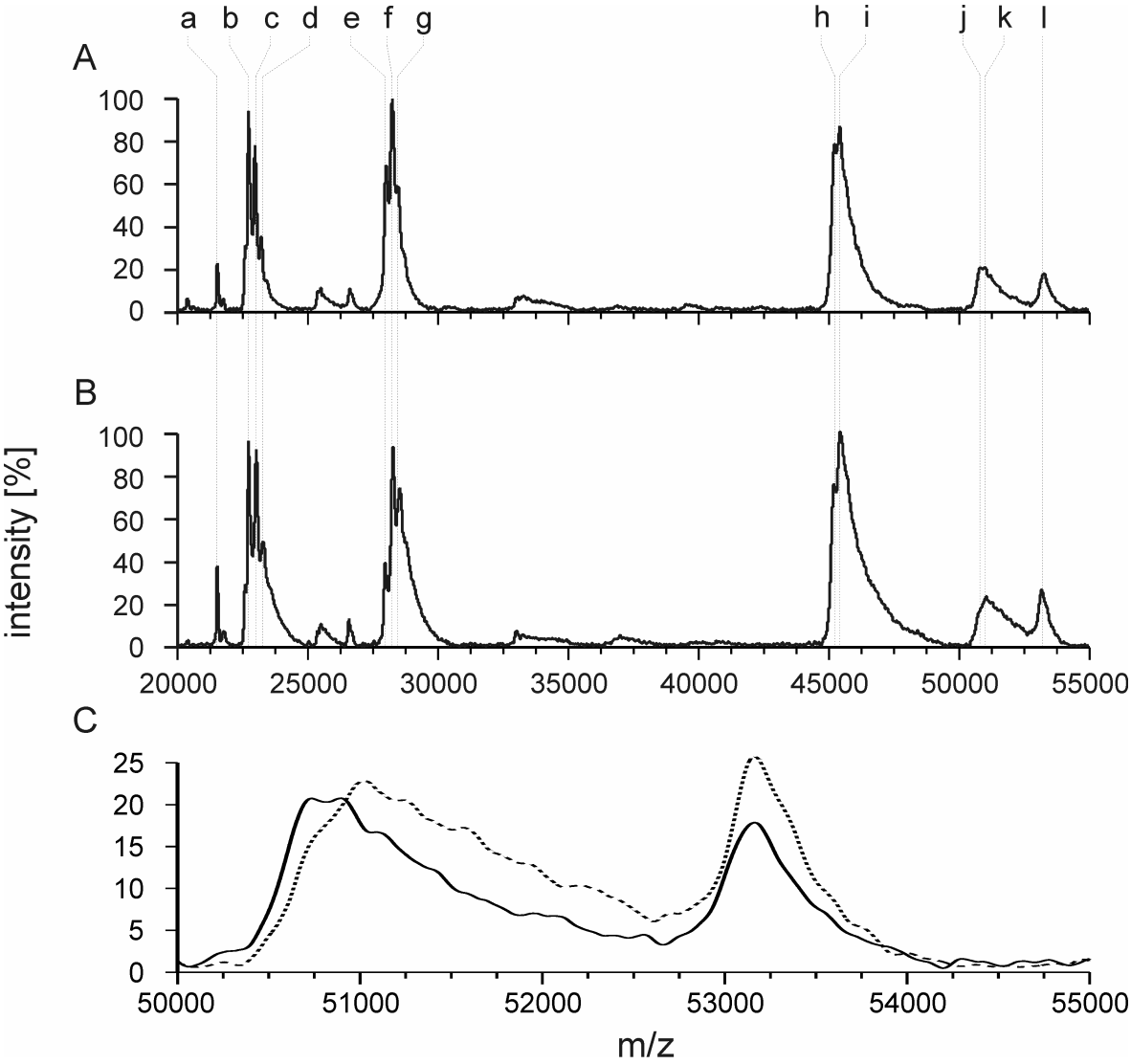

FIGURE S5: Interaction of (A) Q_1 and (B) HQNO with NqrA determined by surface plasmon resonance affinity assays. Steady-state binding levels from two independent dilution series obtained from analyte concentrations up to 3 and 6 µM were fitted to a one-site-binding isotherm.

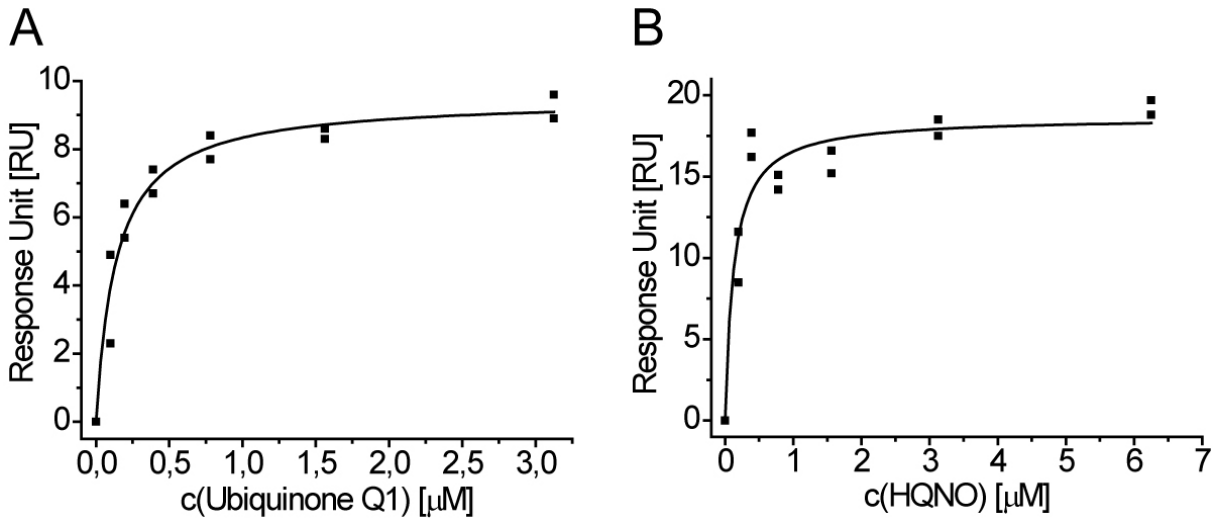

FIGURE S6: SDS-PAGE of NqrA. NqrA after affinity chromatography (4 µg), multimeric NqrA (fraction A, 1 µg) and monomeric NqrA (fraction B, 1 µg) after gel filtration. Proteins were stained with Coomassie.

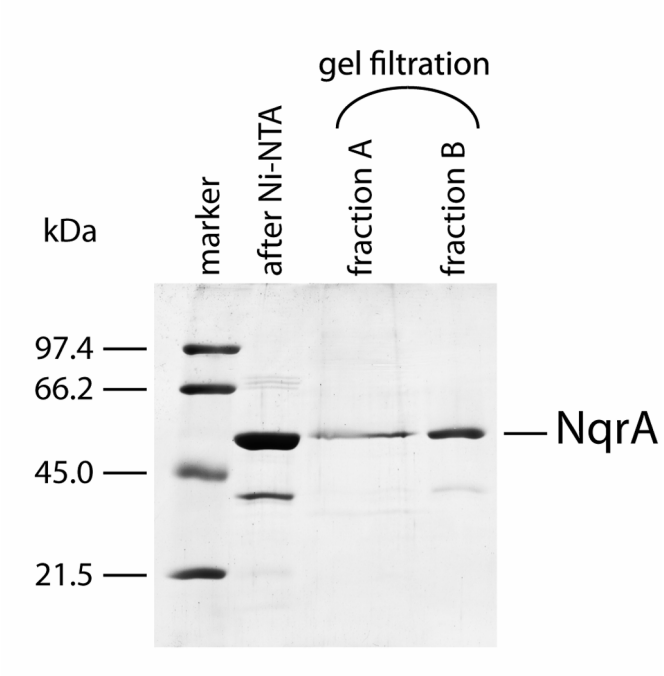

FIGURE S7: STD NMR spectra of Q1 and HQNO in the absence of NqrA. STD NMR spectra of Q1 (panel A) and HQNO (panel B) in the absence of NqrA (upper traces) and in the presence of NqrA (lower traces). The spectra were acquired at identical ligand concentrations and NMR parameters.

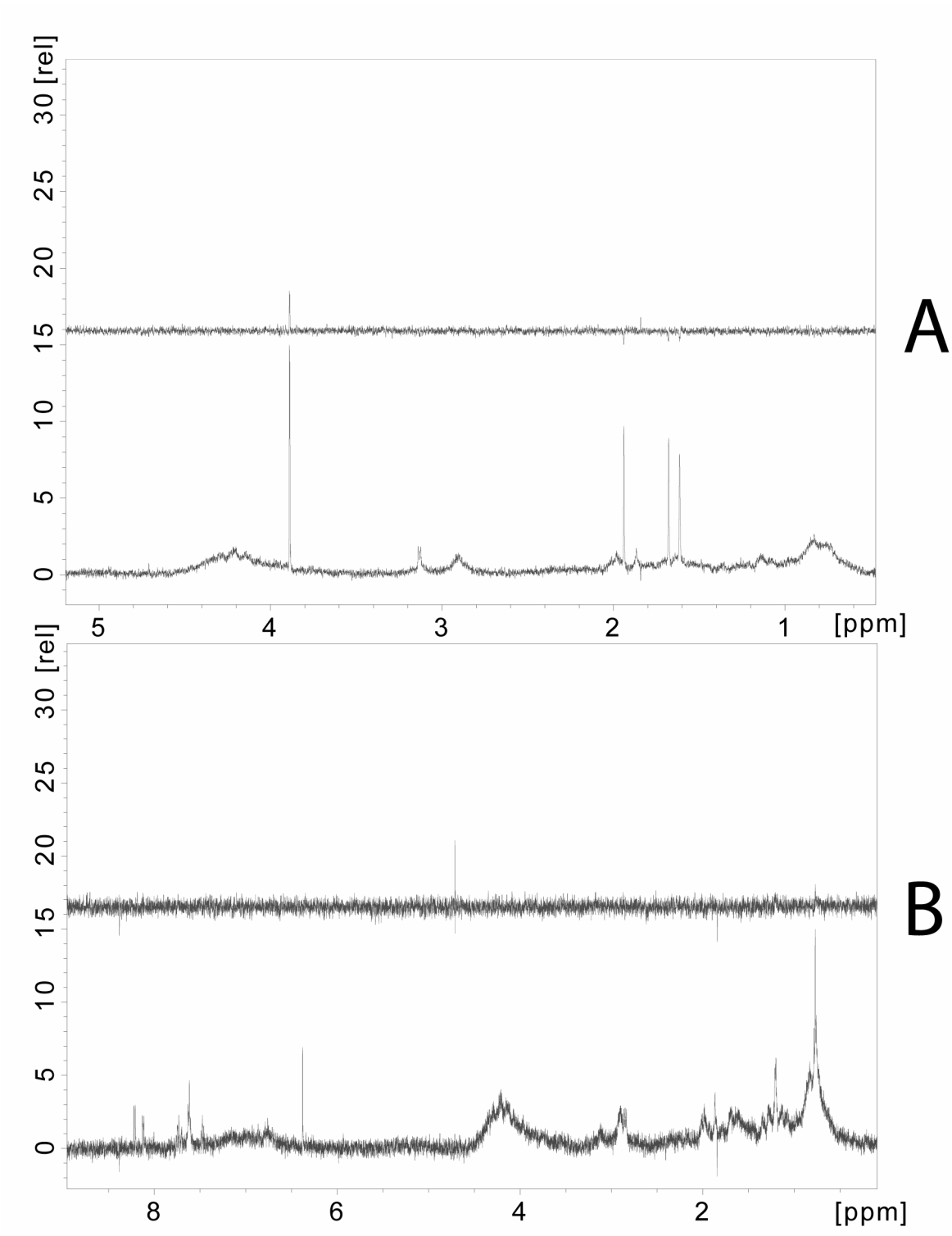

FIGURE S8: STD NMR of riboflavin in the presence of NqrA. Reference NMR spectrum of riboflavin (upper trace) and STD NMR spectra of riboflavin in the presence of NqrA (middle trace) and in the absence of NqrA (lower trace). The molar ratio riboflavin:NqrA was 10:1. The reference spectrum was scaled to 10 % of its original intensity. Signals of the same intensity in the STD spectrum corresponded to an STD effect of 10 %.